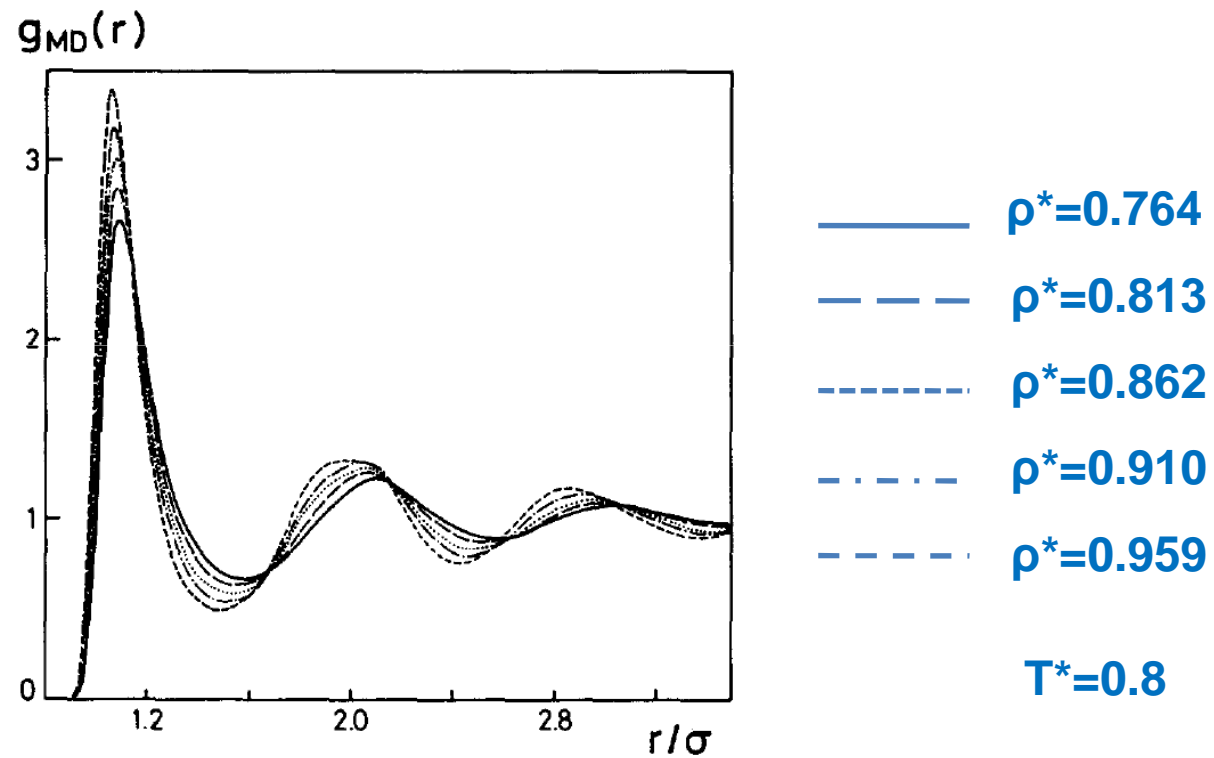
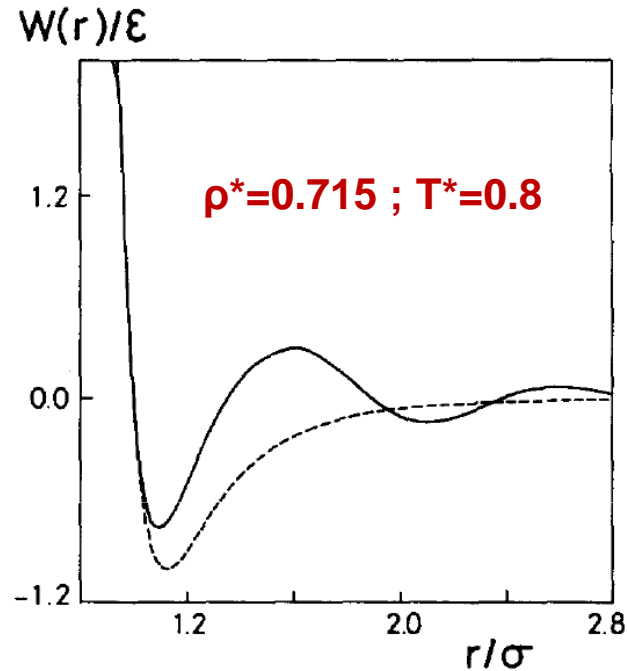


Radial distribution functions for a L-J liquid



E. Guàrdia et al., J. Chem.Phys. 84, 4569 (1986)

Interaction potentials for a L-J liquid



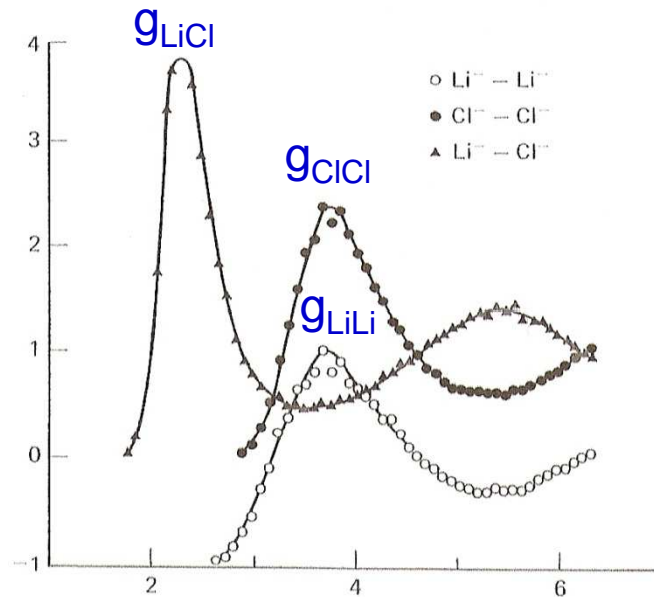
$$U_{LJ}(r) = 4\epsilon \left\{ \left(\frac{\sigma}{r} \right)^{12} - \left(\frac{\sigma}{r} \right)^6 \right\}$$

$$W(r) = -k_B T \ln g(r)$$

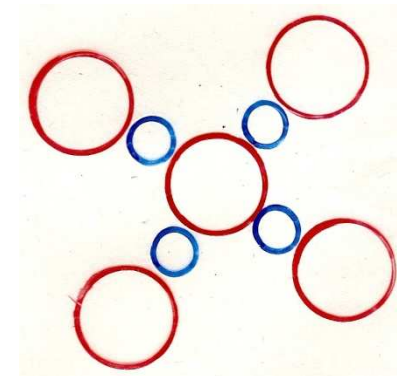
- Lennard-Jones potential
- Mean Force potential

FUNCIONS DE DISTRIBUCIÓ RADIAL PER A LA SAL FOSA LiCl a $T=883\text{K}$, $V=28.3\text{cm}^{-3}$

obtingudes per Monte Carlo amb un potencial d'esferes dures carregades



La posició dels màxims i mínims indica una estructura de capes:

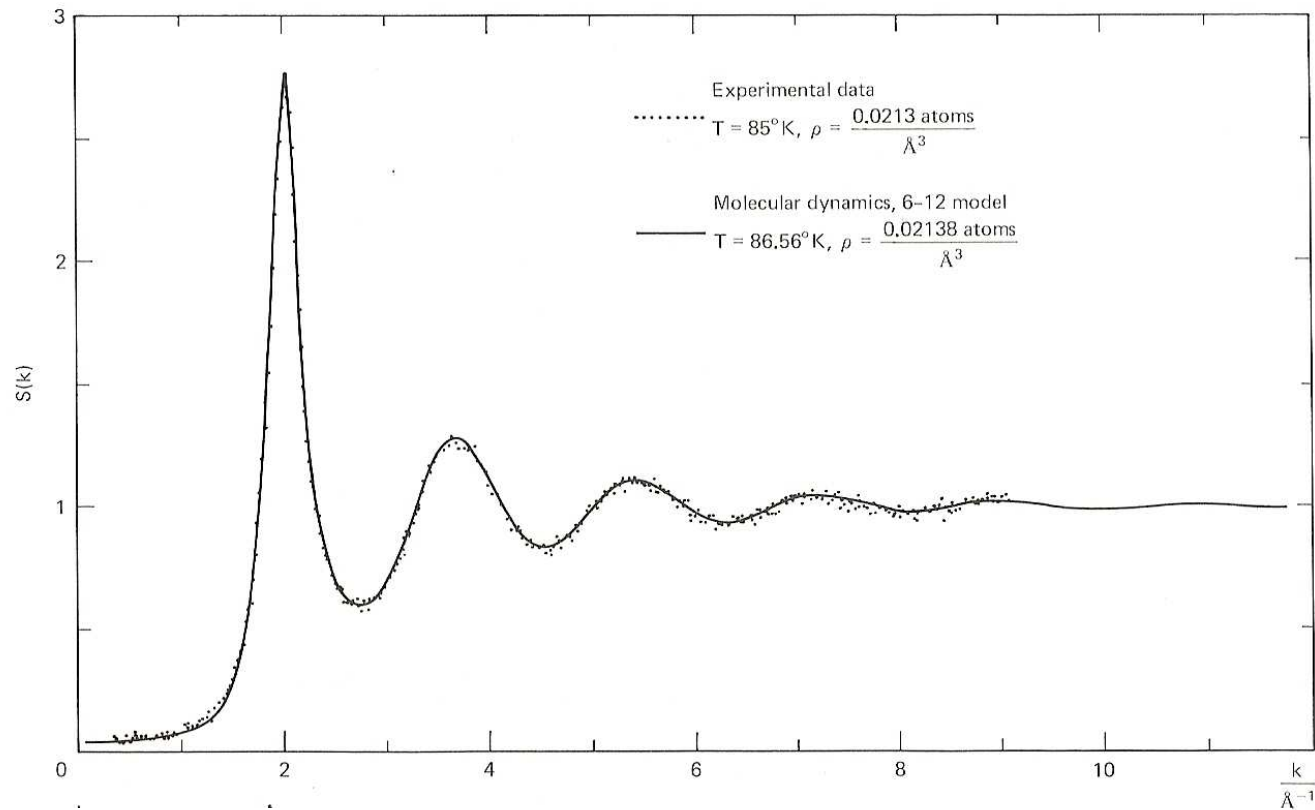


Integrant les $g_{\mu\nu}(r)$ es pot calcular els nombres de coordinació:

$$n_{\mu\nu} = x_{\nu} \int_0^{r_{min}} \rho g_{\mu\nu}(r) 4r^2 dr \quad x_{\nu} = \frac{N_{\nu}}{N}$$

H.L.Friedman, "A Course in Statistical Mechanics", pag.81

FACTOR D'ESTRUCTURA ESTÀTIC Ar LÍQUID



H.L.Friedman, "A Course in Statistical Mechanics", Cap. 5

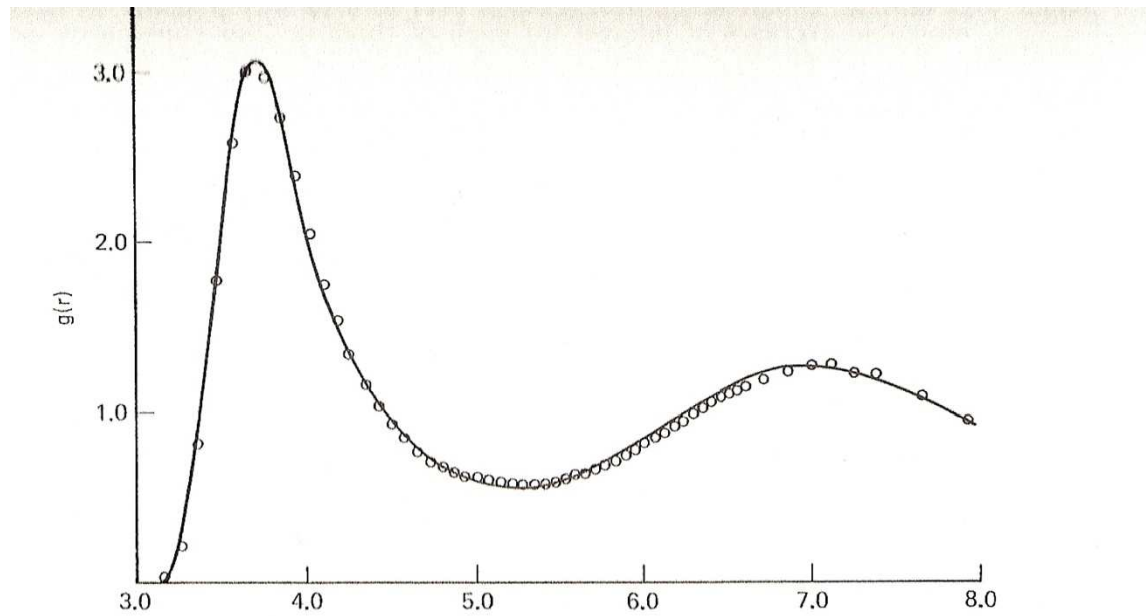
Factor d'estructura i funció de distribució radial

$$S(\vec{k}) = 1 + \rho \int \exp(-i\vec{k} \cdot \vec{r}) g(\vec{r}) d\vec{r}$$

Relació inversa:

$$\rho g(\vec{r}) = \frac{1}{(2\pi)^3} \int \exp(i\vec{k} \cdot \vec{r}) [s(\vec{k}) - 1] d\vec{k}$$

FUNCIÓ DE DISTRIBUCIÓ RADIAL Ar LÍQUID



o o o o o : resultats experimentals

———— : resultats de simulació

A polarizable ion model for the structure of molten AgI

Vicente Bitrián and Joaquim Trullàs^{a)}

*Departament de Física i Enginyeria Nuclear, Universitat Politècnica de Catalunya,
Campus Nord UPC B4-B5, 08034 Barcelona, Spain*

Moises Silbert

School of Mathematics, University of East Anglia, NR4 7QF Norwich, United Kingdom

(Received 13 November 2006; accepted 18 December 2006; published online 11 January 2007)

The results are reported of the molecular dynamics simulations of the coherent static structure factor of molten AgI at 923 K using a polarizable ion model. This model is based on a rigid ion potential, to which the many body interactions due to the anions induced polarization are added. The calculated structure factor is in better agreement with recent neutron diffraction data than that obtained by using simple rigid ion pair potentials. The Voronoi-Delaunay method has been applied to study the relationship between voids in the spatial distribution of cations and the prepeak of the structure factor. © 2007 American Institute of Physics. [DOI: [10.1063/1.2432346](https://doi.org/10.1063/1.2432346)]

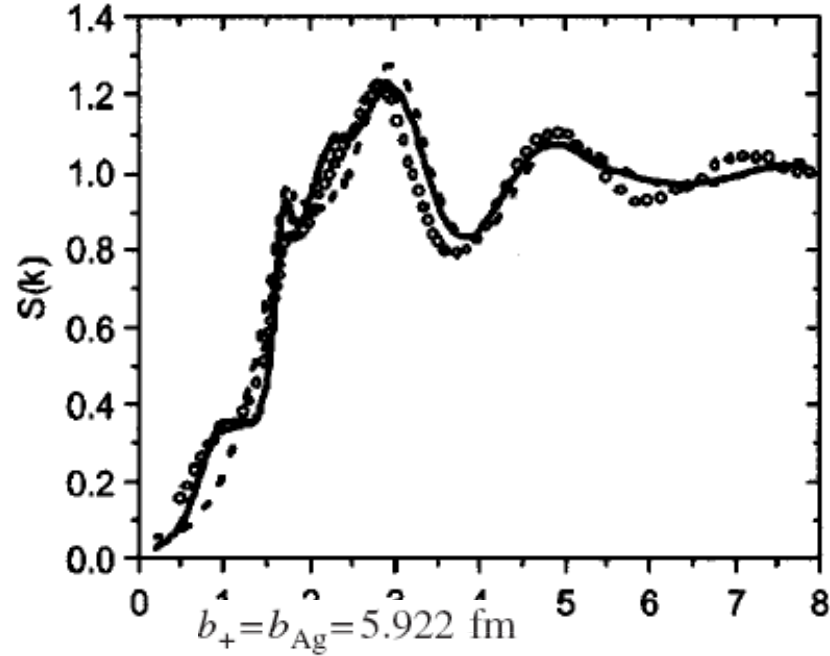


FIG. 1. Coherent static structure factors, $S(k)$, for molten AgI at 923 K from experimental data (open circles), Ref. 20, and MD results using the RIM (dotted line) and the PIM (solid line).

$$S(k) = [b_+^2 S_{++}(k) + b_-^2 S_{--}(k) + 2b_+ b_- S_{+-}(k)] / (b_+^2 + b_-^2)$$

$$b_+ = b_{\text{Ag}} = 5.922 \text{ fm} \quad b_- = b_{\text{I}} = 5.280 \text{ fm}$$

FUNCIONS D'AUTOCORRELACIÓ DE VELOCITATS Ar LÍQUID

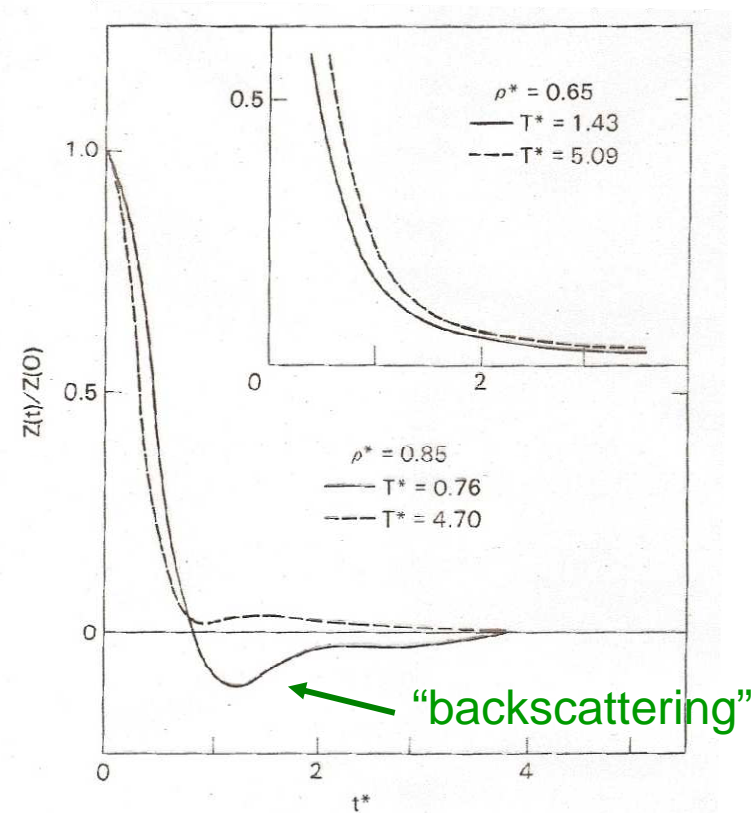


FIG. 7.1. Normalized velocity autocorrelation function of the Lennard-Jones fluid at different reduced temperatures and densities. The unit of time is the quantity τ_0 defined by Eqn. (3.3.5). After Levesque and Verlet (1970).

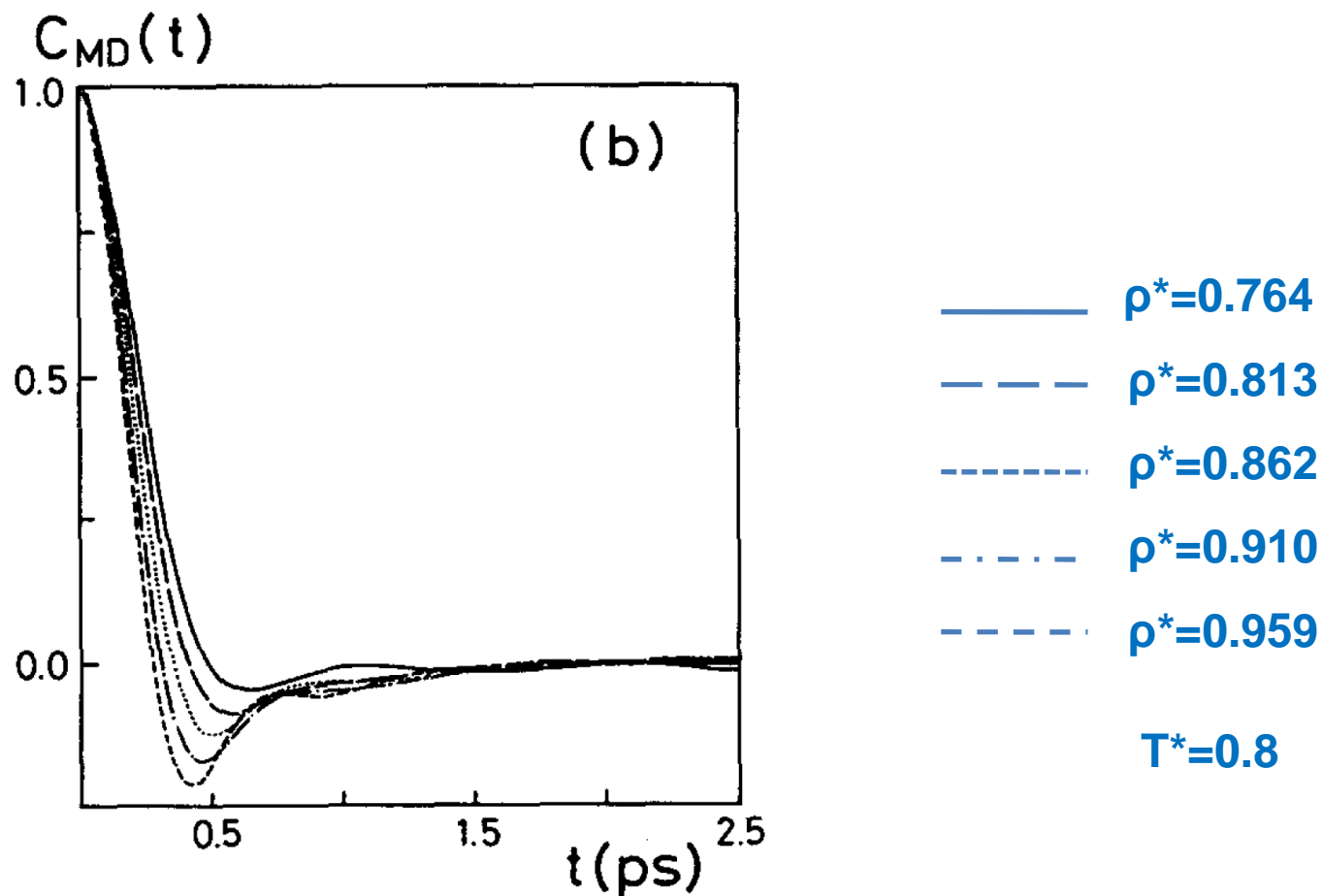
Unitats reduïdes:

$$\rho^* = \rho/\sigma^3$$

$$T^* = K_B T/\epsilon$$

Hansen&McDonald, "Theory of Simple Liquids",

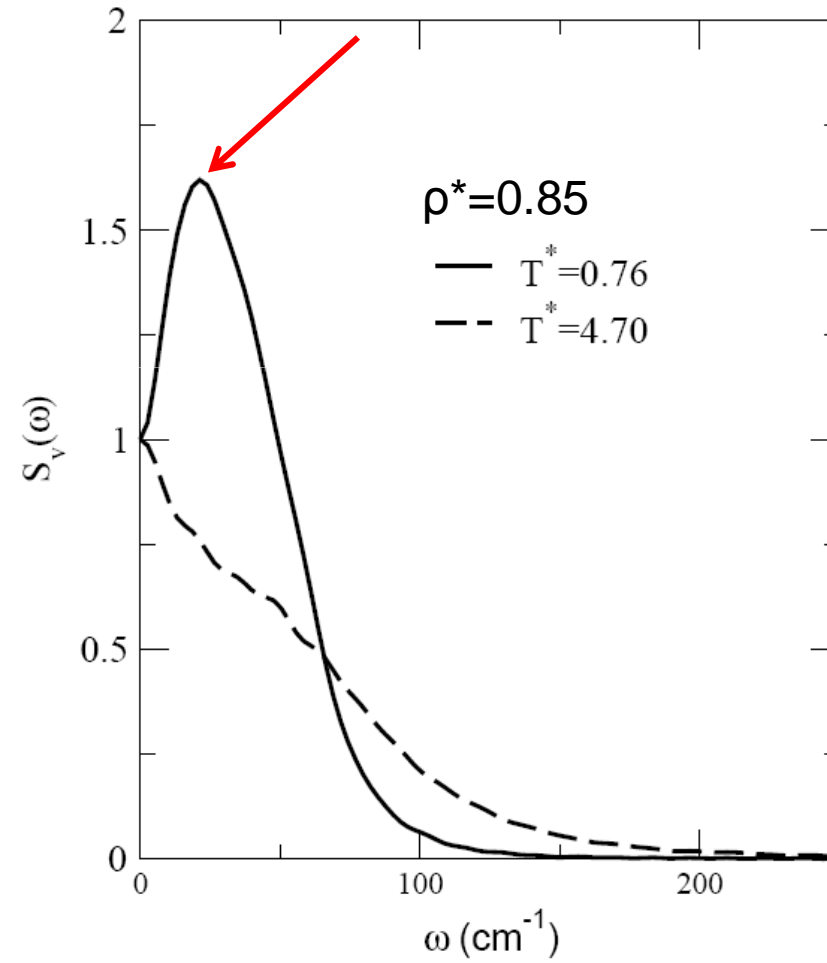
Velocity autocorrelation functions for a L-J liquid

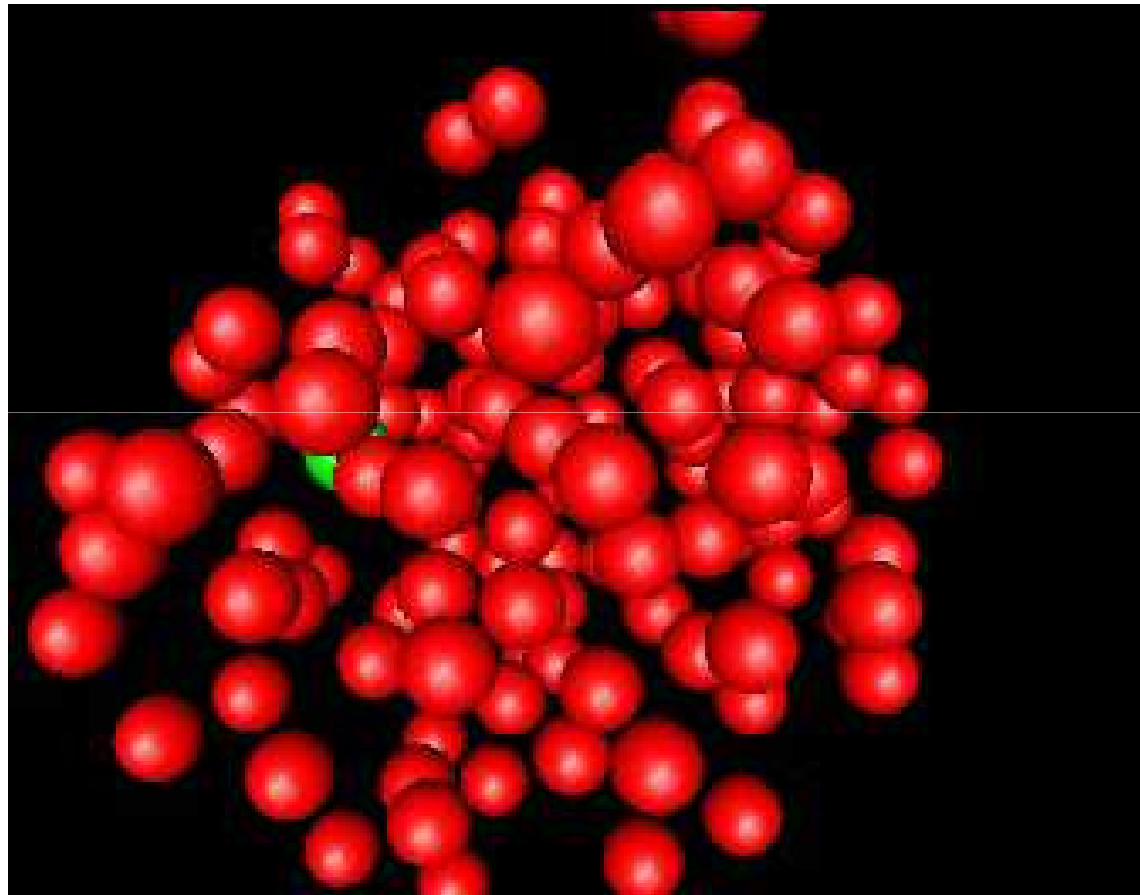


E. Guàrdia et al., J. Chem.Phys. 84, 4569 (1986)

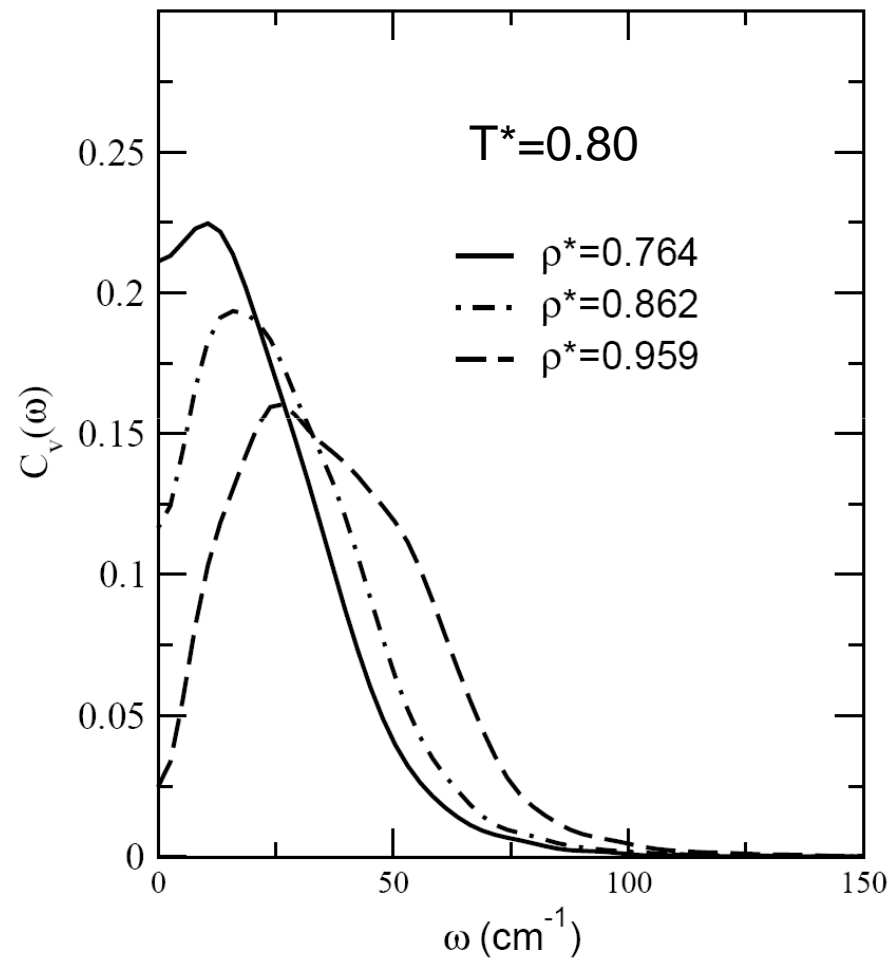
ESPECTRE DE FREQÜENCIES DE LA FUNCIO D'AUTOCORRELACIÓ DE VELOCITATS Ar LÍQUID

"Hindered translations"



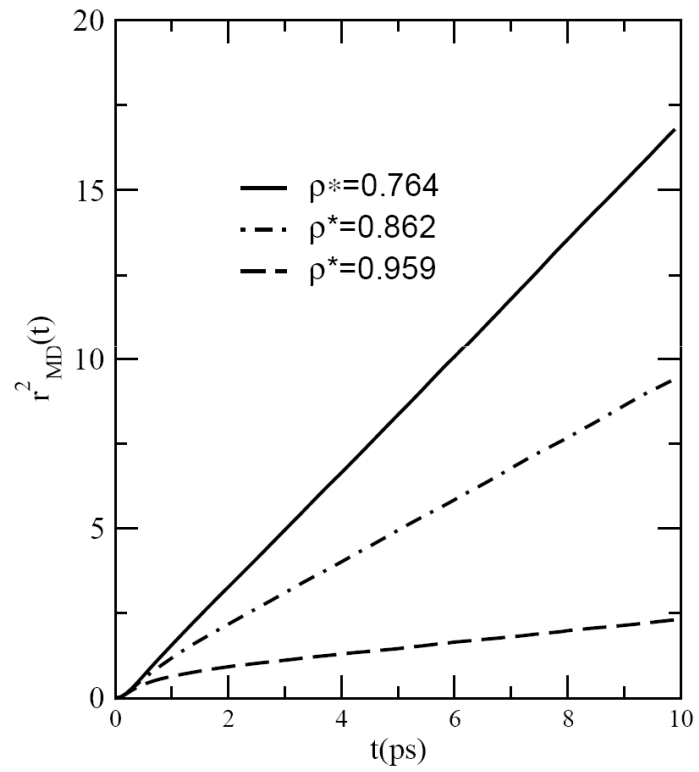


Power spectra of the velocity autocorrelation functions for a L-J liquid



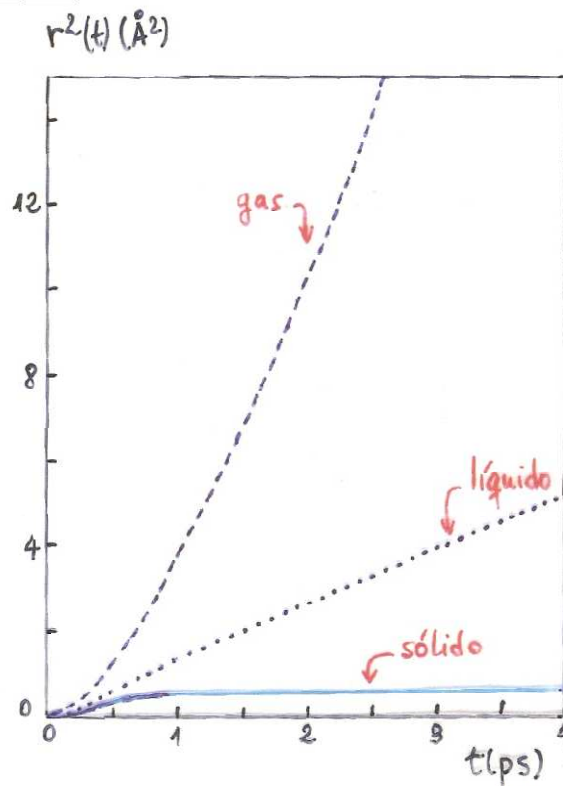
$C_v(0)$: Self-difusion coefficient

Mean square displacement for liquid Kr at $T^*=0.80$



DESPLAÇAMENT QUADRÀTIC MITJÀ Ar

$$r^2(t) = \langle (\vec{r}(t) - \vec{r}(0))^2 \rangle$$



Líquid:

✓ Comportament asimptòtic:

$$r^2(t) \rightarrow 6Dt$$

D: Coeficient d'autodifusió

ESPECTRES DE FREQUÈNCIES PER A L'AIGUA LÍQUIDA ÀTOMS D'HIDROGEN

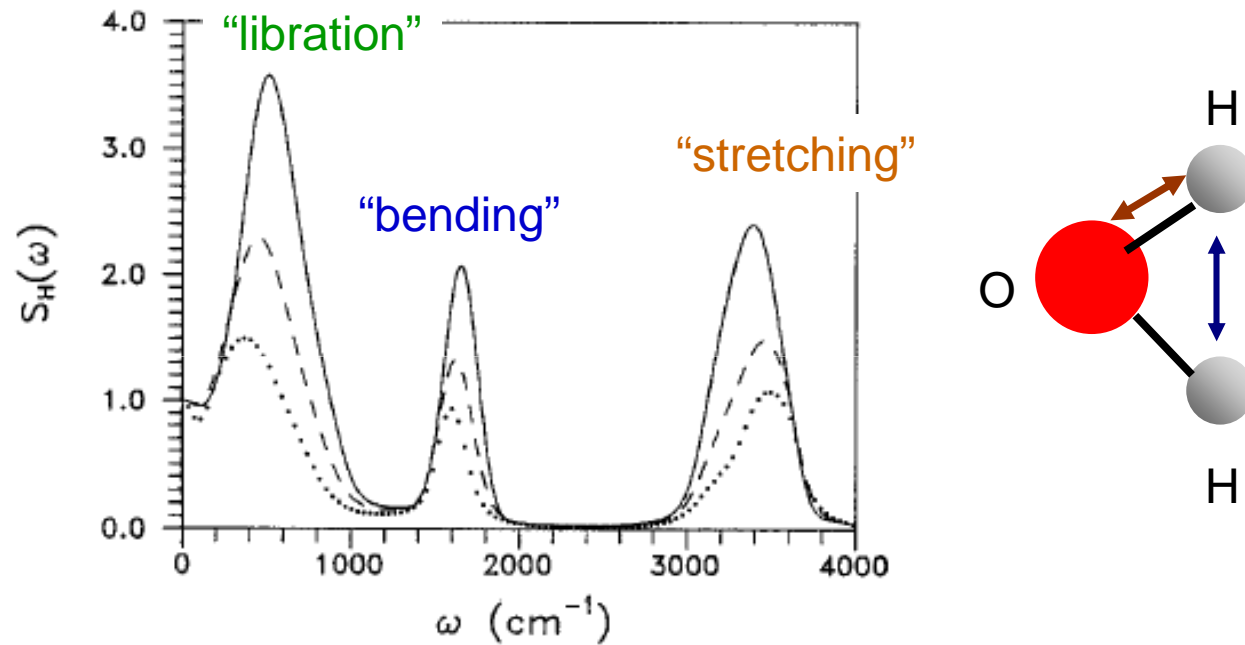
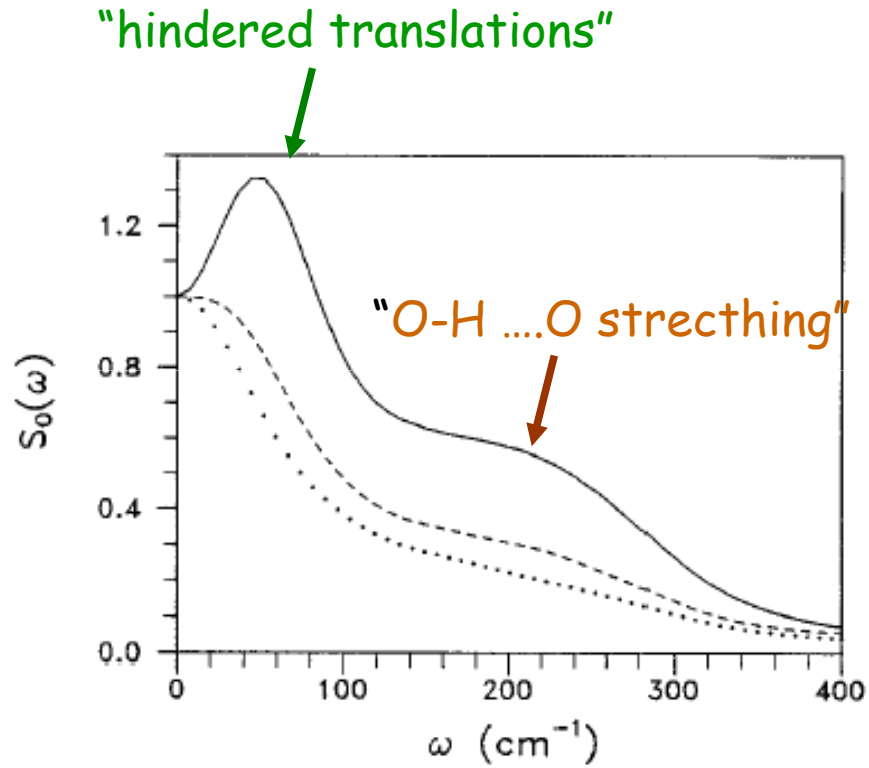


FIG. 11. Normalized hydrogen power spectra for water along the coexistence curve: $T=298\text{ K}$ (—), $T=403\text{ K}$ (---), and $T=523\text{ K}$ (····).

J. Martí, J.A.Padró, E. Guàrdia, J. Chem. Phys. 105, 639 (1996)

ESPECTRES DE FREQUÈNCIES PER A L'AIGUA LÍQUIDA ÀTOMS D'OXÍGEN



Definición geométrica de un puente de hidrógeno

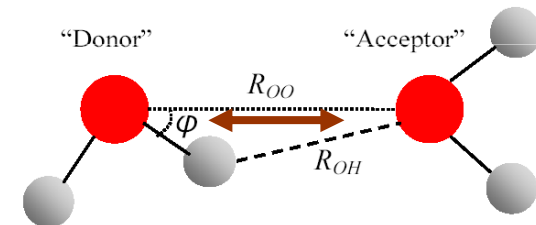


FIG. 8. Normalized $S_O(\omega)$ for water at $\rho=0.91 \text{ g/cm}^3$ and $T=298 \text{ K}$ (—), $T=403 \text{ K}$ (----), and $T=523 \text{ K}$ (.....).

J. Martí, J.A.Padró, E. Guàrdia, J. Chem. Phys. 105, 639 (1996)

FACTOR D'ESTRUCTURA DINÀMIC: COMPORTAMENT QUALITATIU PER A DIFERENTS k

318

16 *Liquid dynamics on the microscopic scale*

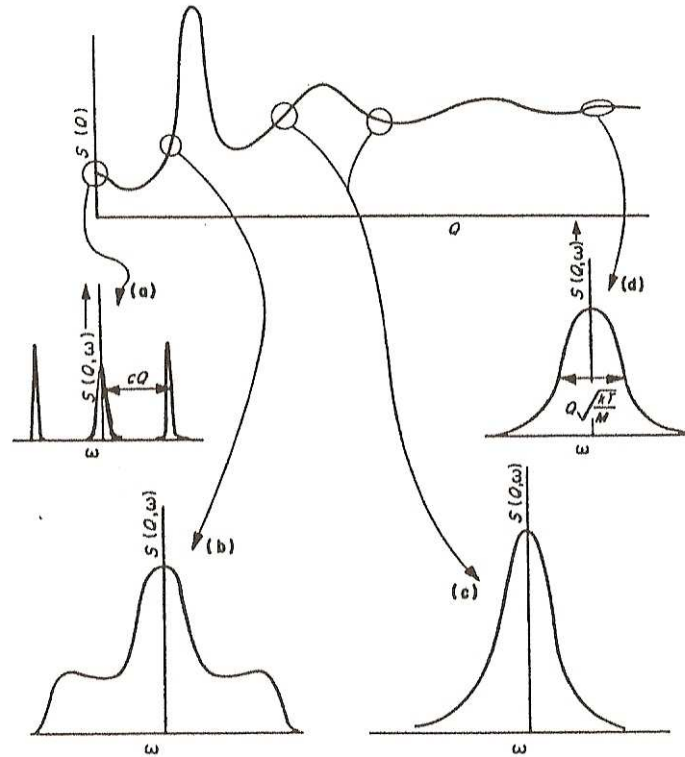


Fig. 16.1 Qualitative behaviour of $S(Q, \omega)$ for several values of Q in the case of a compressible fluid. The upper curve is the function $S(Q)$, and the remaining curves (a) to (d) show the spectral shape at fixed values of Q marked by circles on $S(Q)$. At low and high values of Q , the width can be calculated from simple considerations.

P.A. Egelstaff, "An Introduction to the Liquid State", Clarendon Press 1992

FACTOR D'ESTRUCTURA DINÀMIC LÍMIT HIDRODINÀMIC $k, \omega \rightarrow 0$

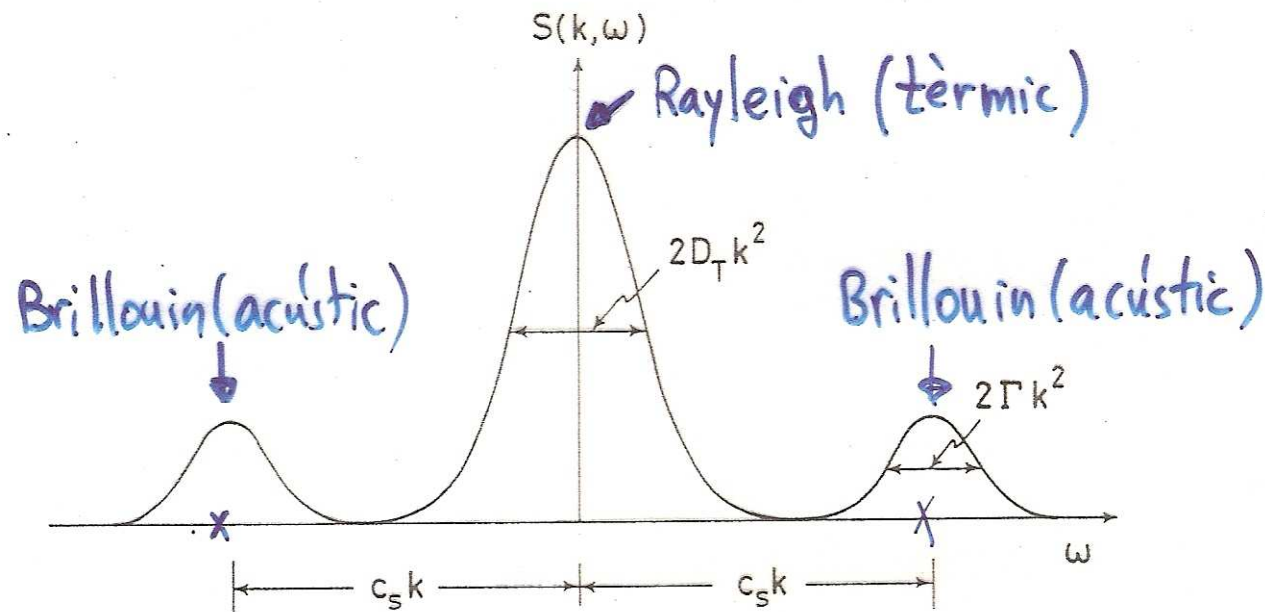


FIG. 8.4. Dynamic structure factor in the hydrodynamic limit; D_T is the thermal diffusivity, Γ is the sound-attenuation coefficient and c_s is the adiabatic speed of sound.

Hansen & McDonald, "Theory of Simple Liquids", Cap. 8

Computer simulation study of liquid lithium at 470 and 843 K

Manel Canales

*Departament de Física i Enginyeria Nuclear, Universitat Politècnica de Catalunya, Mòdul B4, Campus Nord,
Sor Eulàlia d'Anzizu s/n, 08034 Barcelona, Spain*

Luis Enrique González

Departamento de Física Teórica, Universidad de Valladolid, 47011 Valladolid, Spain

Joan Àngel Padró

Departament de Física Fonamental, Universitat de Barcelona, Diagonal 647, 08028 Barcelona, Spain

(Received 20 January 1994)

Both structural and dynamical properties of ${}^7\text{Li}$ at 470 and 843 K are studied by molecular dynamics simulation and the results are compared with the available experimental data. Two effective interatomic potentials are used, i.e., a potential derived from the Ashcroft pseudopotential [Phys. Lett. **23**, 48 (1966)] and a recently proposed potential deduced from the neutral pseudoatom method [J. Phys. Condens. Matter **5**, 4283 (1993)]. Although the shape of the two potential functions is very different, the majority of the properties calculated from them are very similar. The differences among the results using the two interaction models are carefully discussed.

PACS number(s): 61.20.Ja, 61.20.Lc, 61.20.Ne

FACTOR DE SCATTERING INTERMEDIO

$$F(\vec{k}, t) = \frac{1}{N} \langle \rho_{\vec{k}}(t) \rho_{-\vec{k}}(0) \rangle$$

$$\rho_{\vec{k}}(t) = \sum_{i=1}^N \exp(-i\vec{k} \cdot \vec{r}_i(t))$$

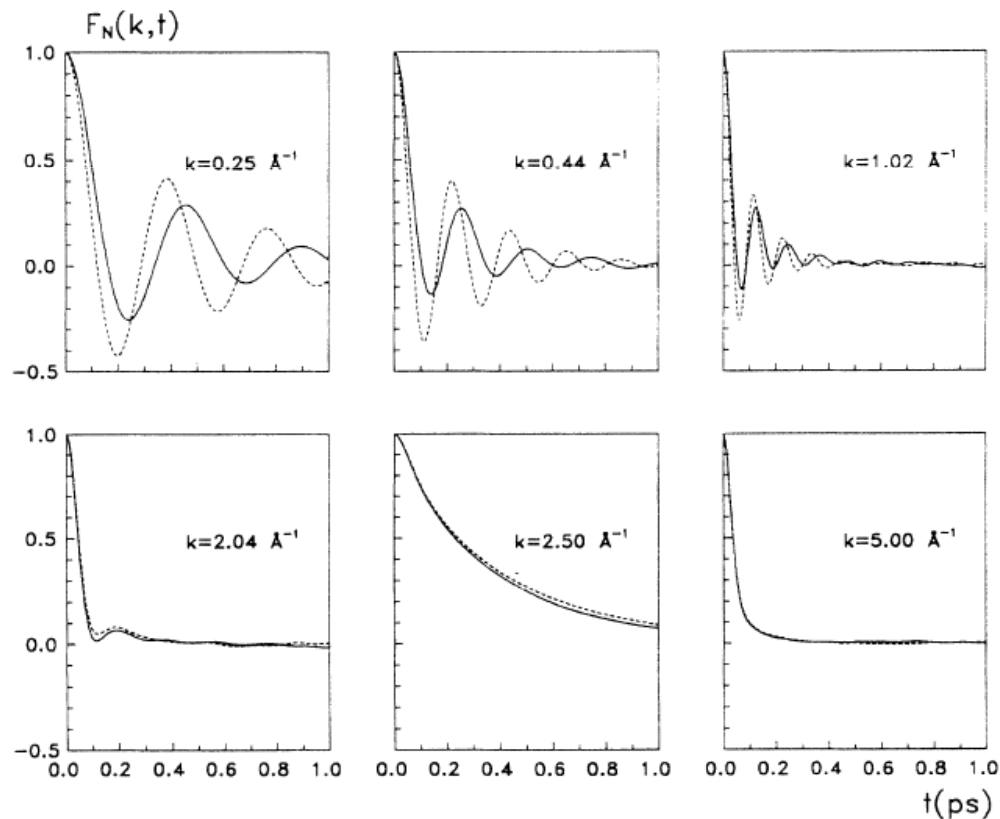


FIG. 7. Normalized intermediate scattering functions at 470 K [REDACTED]. Solid line, NPA potential; dashed line, Ashcroft potential.

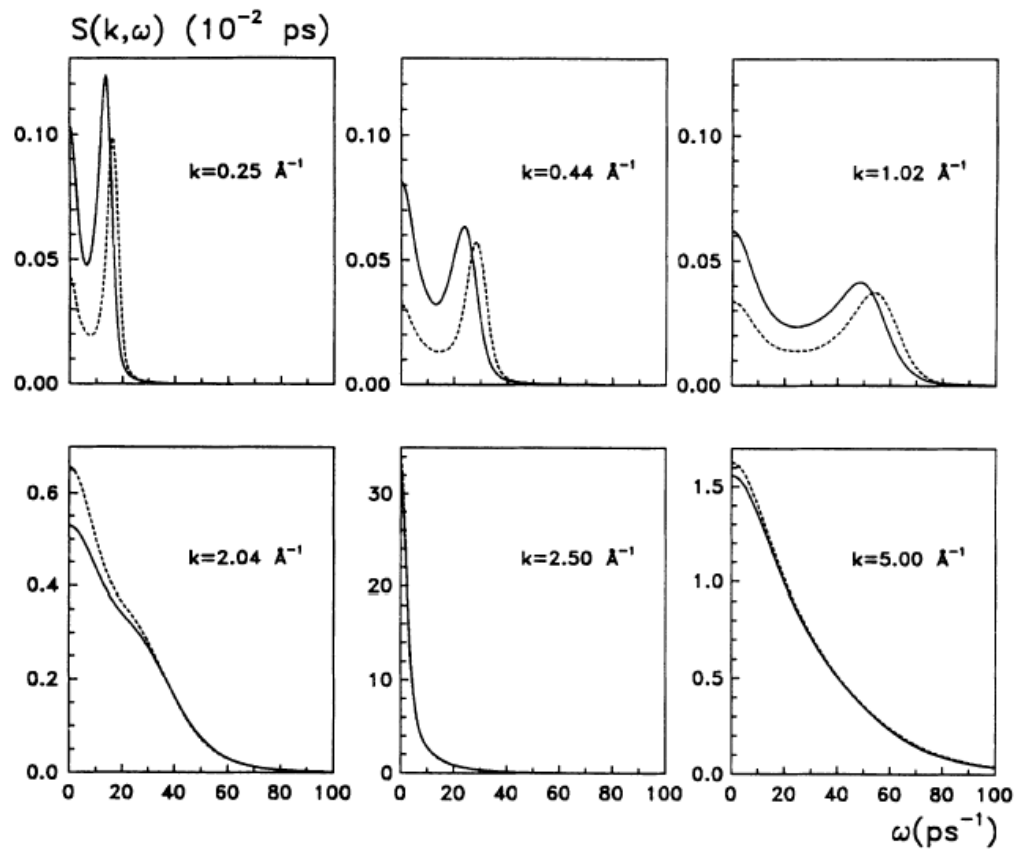


FIG. 11. Dynamic structure factors for different k values at 470 K. Solid line, NPA potential; dashed line, Ashcroft potential.

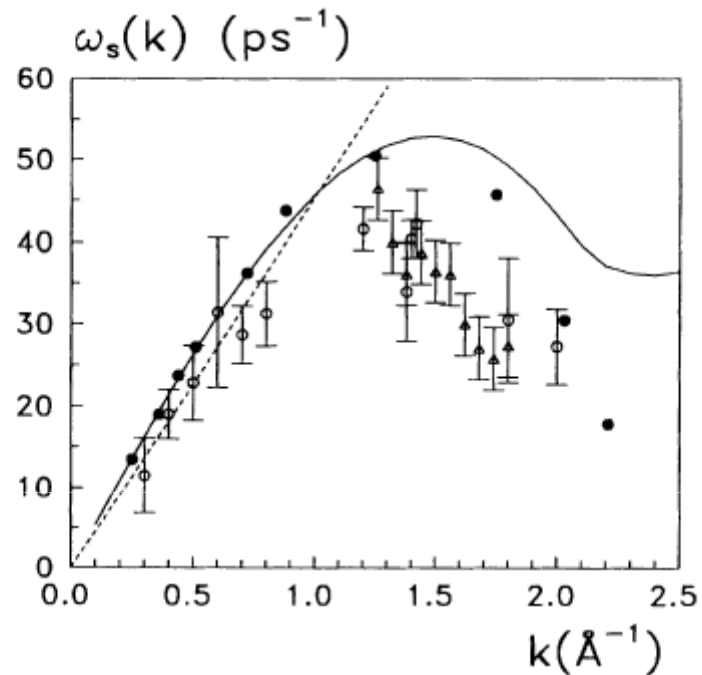


FIG. 14. Sound dispersion relation at 470 K. Solid line, Lovesey viscoelastic model [36]; dashed line, hydrodynamic sound dispersion curve; open circles with error bars, x-ray data [11]; triangles with error bars, neutron scattering data [10]; solid circles, MD results using the NPA potential.

Límite hidrodinámico: $\omega_s = c_s k$